Eclogae geol. Helv. 86/3: 667–692 (1993)

0012-9402/93/030667-26 $1.50 + 0.20/0
Birkhäuser Verlag, Basel

Thermal maturity and modelling of Mesozoic and Cenozoic sediments in the south of the Rhine Graben and the Eastern Jura (Switzerland) [1]

By IVAYLO TODOROV [2], ROLAND SCHEGG [3] & WALTER WILDI [3]

Key words: Vitrinite reflectance, Rock-Eval pyrolysis, thermal modelling, Rhine Graben, foreland basin, Molasse basin, convective heat transport

ABSTRACT

The aim of our study is to reconstruct the thermal history in a region situated at the intersection of the extension dominated Rhine Graben and the compression dominated realm of the eastern Jura mountain belt. Outcrop and well samples from Mesozoic shales and siltstones, as well as phytoclast-rich Tertiary sandstones have been collected. In order to determine the maturation level of these samples, the vitrinite reflectance of dispersed organic matter and of phytoclasts has been measured. Vitrinite reflectance values vary between 0.24% Rr and 0.54% Rr for Tertiary, between 0.40% Rr and 0.70% Rr for Jurassic, and between 0.49% Rr and 0.80% Rr for Upper Triassic formations. Rock-Eval anaylsis results confirm vitrinite reflectance data. Some of the studied formations (e.g. Posidonia Schiefer) appear to contain oil prone source rocks.

Thermal modelling of the measured maturity data indicates that the present maturation level of the Mesozoic and Cenozoic formations has probably been attained during a Tertiary high temperature regime. The computed maximum paleogeothermal gradients in the study area range from 40 to 100 °C/km. The calculated maximum paleotemperatures vary from 53 to 106 °C for Jurassic and from 77 to 127 °C for Triassic formations. One hypothesis to explain the postulated Tertiary high temperature regime is an enhanced regional heat flow due to convective heat transport. This may be the result of the migration of "hot" fluids from greater depth along faults zones (especially during the extensional period between Late Eocene and Late Miocene).

RÉSUMÉ

Le but de cette étude est une reconstitution de l'histoire thermique de la région située à l'intersection entre le Fossé rhénan, formé par extension au cours du Tertiaire, et le Jura oriental, dominé par la compression. Cette reconstitution repose sur une analyse de la maturité de la matière organique dispersée, déterminée par la mesure de la réflectance de la vitrinite, sur des échantillons provenant d'affleurements et de forages. Les principales lithologies concernées sont des pélites d'âge mésozoïque et des grès tertiaires riches en débris de plantes. Les valeurs de réflectance de la vitrinite varient entre 0.24% Rr et 0.54% Rr pour les sédiments du Tertiaire, entre 0.40% Rr et 0.70% Rr pour le Jurassique, et entre 0.49% Rr et 0.80% Rr pour le Trias supérieur. Les analyses de pyrolyse Rock-Eval confirment ces valeurs. Certaines formations, et notamment les schistes à posidonies, apparaissent comme des roches mères.

La modélisation thermique de la maturité mesurée indique que celle-ci a été atteinte au cours d'une phase de haute température au Tertiaire. Les paléogradients thermiques varient entre 40 et 100 °C/km. Les paléotempératures maximales calculées varient entre 53 °C et 106 °C pour le Jurassique et entre 77 °C et 127 °C pour les

[1] Swiss National Foundation for Scientific research projects n° 20-30-89491 and 20-26218.89

[2] Present address: Omurtag 8, 1124 Sofia, Bulgaria

[3] Département de Géologie et Paléontologie, 13 rue des Maraîchers, CH-1211 Genève 4, Switzerland.

formations du Trias. Une hypothèse possible pour expliquer le système de haute température postulé pour le Tertiaire est un flux de chaleur par convection, notamment par la migration de fluides profonds circulant le long d'accidents tectoniques, particulièrement pendant les périodes d'extension de l'Eocène supérieur au Miocène supérieur.

1. Introduction and geological setting

In north-eastern Switzerland, two geothermal anomalies are determined by major basement structures which are (1) the southern termination of the N-S running Cenozoic Rhine Graben, and (2) the eastern part of the E-W striking late Palaeozoic Constance-Frick-Lons le Saunier trough (Fig. 1):

(1) The Rhine Graben is a well developed intracontinental rift extending from Mainz in the NNE to Basel in the SSW, separating the elevated Hercynian blocks of the Vosges in the W from the Black Forest in the E (Illies 1974). Starting in Middle Eocene, this rift

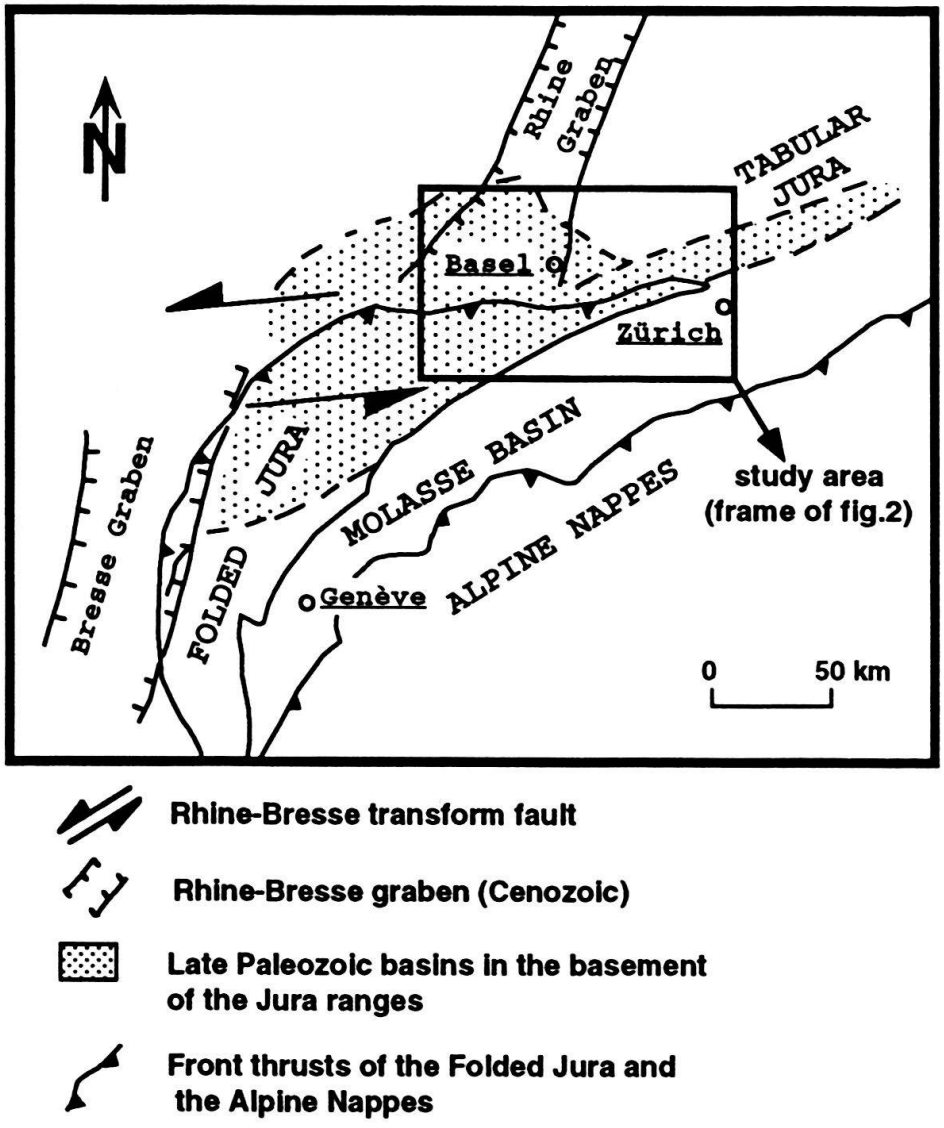

Fig. 1. Major tectonic trends of the Alpine Foreland, relationship between basement and cover.

basin subsided with major phases of geothermal flux during Eocene-Oligocene and from the Pliocene to the present (Teichmüller & Teichmüller 1979, see also Robert 1985, p. 191–213). Modern geothermal gradients are about 50 °C/km in Basel, with a decrease towards the S, E and W, and an increase towards the N (Rybach et al. 1987). South of Basel, the Graben structure degenerates into a simple flexure at its eastern border. Numerous narrow grabens, normal faults and left-lateral strike-slip faults extend SSW-wards into the epivariscan Mesozoic cover of the Tabular Jura and the folds and thrusts of the Folded Jura (e.g., Laubscher 1982, 1986, 1987, 1992). The main graben structure is in fact a pull apart basin linked to the Bresse Graben further W by a transform fault zone (Lacombe et al. 1990).

(2) This transform fault zone coincides partly with the strike-slip and graben structure of the late Palaeozoic Constance-Frick-Lons le Saunier trough, which is known since a long time in the basement of the western Jura (Debeglia & Gable 1984, cum biblio.), and which has been described in the eastern Jura by Müller et al. (1984), Laubscher (1987) and Diebold et al. (1991). The stratigraphic record and the tectonic structure as deduced from reflection seismics indicate Late Paleozoic subsidence due to strike-slip movements. In NE Switzerland, the décollement of the Folded Jura coincides with the southern margin of this trough. Therefore, Laubscher (op. cit.) suggests a remobilisation of this margin during the Tertiary. A geothermal anomaly with gradients up to 50 °C/km is indicated along this trough (from Lake Constance to the lower Aare valley) by thermal springs and by heat flow measurements in deep wells (Rybach et al. 1987, Griesser & Rybach 1989).

Whereas the geothermal history of the Rhine Graben has been reconstructed with the help of maturation studies of organic matter in sediments (e.g. Teichmüller & Teichmüller 1979), little data are available for the reconstruction of the temperature evolution south of the Rhine Graben (Wolf & Hagemann 1987). Vitrinite reflectance measurements in deep wells of Northern Switzerland have mainly contributed to the reconstruction of the Late Hercynian temperature history (Kempter 1987). A fluid inclusion study in the same wells (Mullis 1987) gives, however, some indications on the thermal regime during the Tertiary.

The aim of this study is to analyse the maturity of Mesozoic and Cenozoic sediments in an area situated at the intersection of two major basement structures in order to reconstruct its geothermal history. An important aspect of this reconstitution is to look for links between the thermal evolution and the basement structures. The latter control for instance the present-day thermal anomalies of Northern Switzerland.

2. Rock samples

54 samples from outcrops and shallow coreholes of Mesozoic and Tertiary formations (Fig. 2) have been collected for this study. Tertiary samples consist mainly of vitritic phytoclasts. These macroscopic coaly particles (branches, stems, ...) are most probably fragments of the woody material which was often washed into the sedimentary environment of the Molasse rocks. Mesozoic samples comprise shales and marlstones with a relatively high content of dispersed organic matter (OM). Samples were selected from various sites in order to investigate a complete stratigraphic sequence.

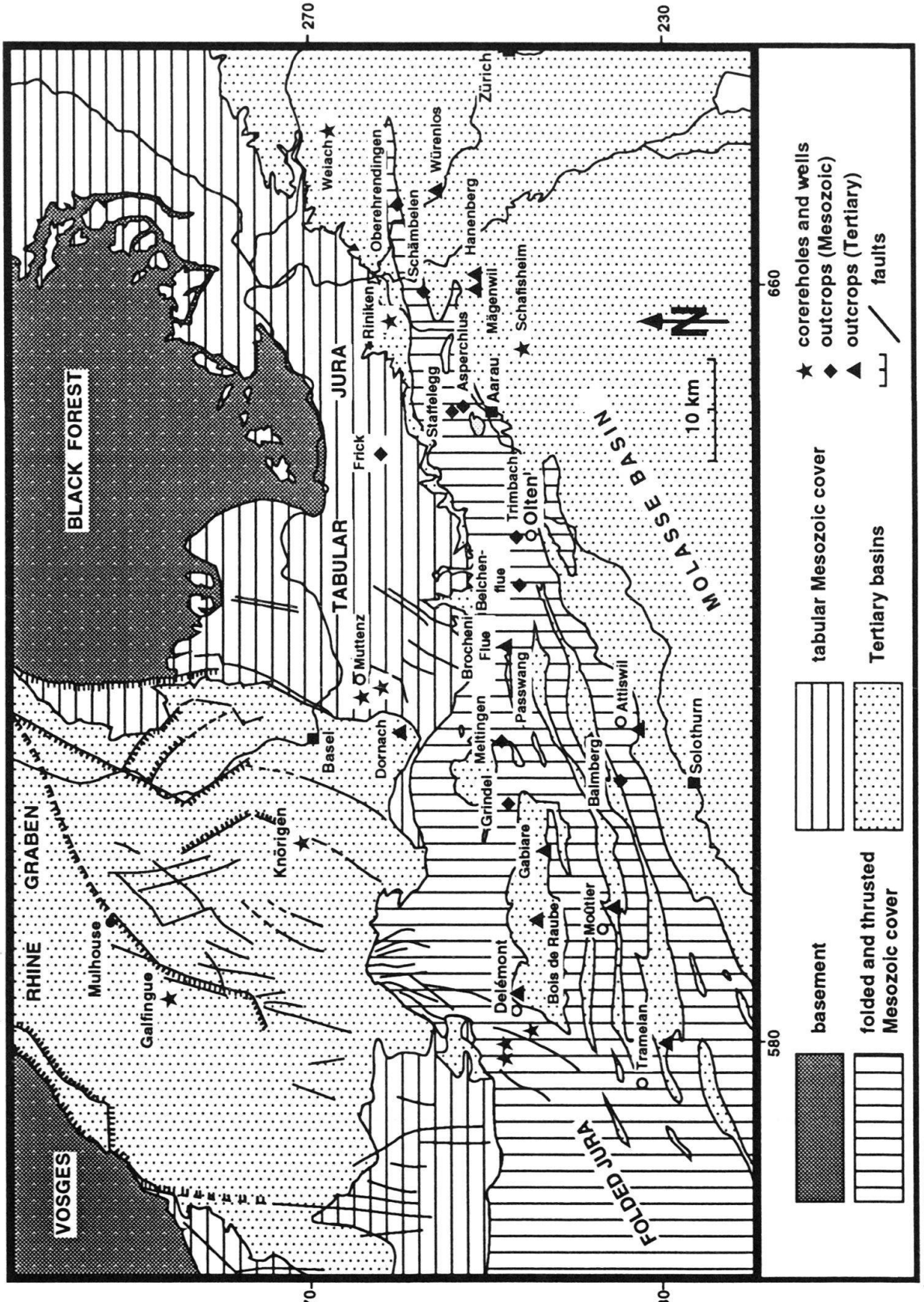
270
230
BLACK FOREST
VOSGES
RHINE GRABEN
JURA
TABULAR
FOLDED JURA
MOLASSE BASIN
Mulhouse
Galfingue
Knörigen
Basel
Muttenz
Frick
Dornach
Weiach
Oberehrendingen
Riniken
Schambelen
Würenlos
Zürich
Hanenberg
Mägenwil
Schafisheim
Staffelegg
Asperchlus
Aarau
Trimbach
Olten
Brochen
Flue
Beichen-
flue
Passwang
Grindel
Meltingen
Gabiare
Balmberg
Attiswil
Solothurn
Delémont
Bois de Raube
Moutier
Tramelan
580
660
10 km
N
basement
folded and thrusted Mesozoic cover
tabular Mesozoic cover
Tertiary basins
corereholes and wells
outcrops (Mesozoic)
outcrops (Tertiary)
faults

3. Preparation and measurement techniques

3.1 Sample preparation

Three types of preparations were used for the dispersed organic matter:

a) Whole rock polished sections: Dried outcrop and corehole samples were mounted in epoxy resin, then ground and polished with different diamond sprays (6, 3, 1, 0.25 μm). The sections were cut perpendicular to bedding. This type of preparation enables to analyse the relationships between organic and inorganic compounds, and therefore, helps to distinguish indigenous and reworked organic material. Fresh (first-cycle) humodetrinite (vitrodetrinite for higher ranks) originates mainly from washed-in woody fragments, whereas reworked (second-cycle) material originates from organic particles that have been eroded from older sedimentary strata (Lo 1992). Whole rock polished section technique does not affect the optical properties of the organic matter, but it can only be used when the samples comprise sufficient vitrinite for reflectance measurements.

b) Polished concentrated organic sections: Samples were crushed to about 150 μm in size, then the organic matter was concentrated by a sink-float method (centrifuging in aqueous zinc bromide) according to the procedure described by Barker & Pawlewicz (1986). The dried concentrate was mounted in epoxy resin and polished as described above. This type of preparation allows a relatively rapid concentration of the organic matter and does not affect the optical properties of their constituents. This technique was used for samples relatively rich in organic matter.

c) Polished isolated kerogen sections: The kerogen concentrates were obtained by using HCL/HF digestion of the rock matrix following the procedure described by Creaney (1980). This technqiue was used for samples lean in organic matter.

Macroscopic organic matter was prepared using the following method:

d) Pellets of particulate coal: Phytoclasts were separated from the host rock, crushed to a particle size between 0.4 and 1 mm, mounted in epoxy resin, then ground and polished as described above.

3.2 Measurement techniques

Fluorescence microscopy

All polished samples (organic and kerogen concentrates, as well as whole rock samples) were observed during ultra-violet irradiation. A Leitz MPV compact microscope with an ultra high pressure 100 W mercury lamp was used to provide the excitation. The observation under UV-irradiation enables to identify the liptinites and to distinguish them from the mineral matrix or from other macerals.

Reflected white light microscopy

Mean random vitrinite reflectance (Rr) was determined in white light at a wave length of 546 nm and a measuring aperture size of 4 μm using a Leitz MPV compact micro-

Fig. 2. Tectonic map of the study area with location of sample sites (outcrops, coreholes and wells)

scope. The measurements followed the procedure described by Stach et al. (1992). The results were generally obtained from at least 50 measurements, where sufficient "true vitrinites" (Durand et al. 1986) were present. The use of dispersed organic matter in maturity determination of sedimentary rocks can introduce uncertainties which are related with the choice of particles for measurements (see Stach et al. 1982 for a review). Uncertainties are reflected in a large scattering of the vitrinite reflectance histograms. In order to avoid these identification difficulties, polished, untreated samples were preferred as far as possible, because recycled or oxidised vitrodetrinites are easier to identify in whole rock samples than in concentrates.

Organic geochemistry

Most of the Mesozoic samples were analysed by Rock-Eval pyrolysis (for a review of the method see Espitalié et al., 1985a, 1985b, 1986). The analyses were performed by the Institut Français du Pétrole in Paris. Values for total organic carbon (TOC), hydrogen index (HI), oxygen index (OI) and the maximum pyrolysis temperature (Tmax) were obtained. Kerogen types I, II and III are those described by Tissot and Welte (1984).

4. Vitrinite reflectance

The results of vitrinite reflectance measurements are summarised in the stratigraphic order of the samples (Table 1, Fig. 3).

4.1 Tertiary

Mean random vitrinite reflectances (Rr) of 6 Miocene and 7 Oligocene samples have been determined. The vitrinite reflectance values for the Miocene sediments range between 0.24% Rr for a sample of the Upper Freshwater Molasse (OSM) and 0.52% Rr for a sample of the Upper Marine Molasse (OMM).

The Rr values for the Oligocene samples vary from 0.30% Rr to 0.81% Rr. The latter value is surprisingly high. A detailed petrographical observation of this sample revealed the presence of recycled and oxidised vitrinite. According to Durand et al. (1986), the organic material in sandstones is very likely to be weathered. Marchioni (1983) documented an increase of reflectance in low-rank coals and a decrease of reflectance in bituminous coals with increased weathering. Therefore, this sample was not used for the interpretation of the data.

The maturity of Tertiary sediments varies geographically (Fig. 3). Samples in the western part of the study area are immature (0.24–0.28% Rr). To the east, in a region situated in the southern prolongation of the eastern Rhine Graben border, vitrinite reflectance increases to values of up to 0.55% Rr. A consecutive decrease in the maturity of the Tertiary sediments towards the eastern termination of the Folded Jura seems to be indicated by an immature sample from the Lower Freshwater Molasse (RS223, 0.30% Rr). Samples from the Molasse basin (s.s.) situated in the eastern part of the study area display again rather high vitrinite reflectance values (0.40–0.52% Rr).

Sample,N°	Location	Y-Coord.	X-Coord.	Age	Stratigraphy	TOC	HI	OI	Tmax	%Rr	S	N	PM
MIOCENE													
Weid96	Tramelan	230000	580000	Tortonian	OSM					0.28	0.04	50	4
RS224	Bois de Raube	246450	585100	Serravallian	Vogesenschotter					0.24	0.02	50	4
RS226	Mägenwil	251075	660550	Burdigalian	OMM					0.44	0.04	50	4
RS297	Hanenberg	251150	661300	Burdigalian	OMM					0.40	0.05	50	4
RS300	Mägenwil	251050	659950	Burdigalian	OMM					0.52	0.04	50	4
RS311	Würenlos	255700	669650	Burdigalian	OMM					0.44	0.03	50	4
OLIGOCENE													
RS223	Brocheni Flue	247550	621900	Chattian	USM					0.30	0.02	50	4
Weid2	Dornachbrugg 2	259840	612660	Chattian	Molasse alsacienne					0.41	0.03	97	4
Weid80	Attiswil	233000	613000	Chattian	USM					0.81	0.07	50	4
Weid97	Gabiare	243090	600140	Chattian	Molasse alsacienne					0.50	0.04	50	4
Weid112	Moûtier	235600	594290	Chattian	Molasse alsacienne					0.54	0.07	50	4
Weid119	Delémont	244510	592880	Chattian	Molasse alsacienne					0.41	0.05	50	4
Weid120	Delémont	244510	592880	Rupelian	UMM s.l.					0.49	0.04	68	4
LATE JURASSIC													
IT3	Oberehrendingen	261000	668500	Oxfordian	Effinger Schichten	0.11	29	143	433	0.49	0.09	58	3
MIDDLE JURASSIC													
IT10	Asperchlus	252800	647400	Bathonian	Hauptrogenstein					0.40	0.04	72	4
IT13	Meltingen	248300	612000	Aalenian	Opalinus Ton	0.69	65	94	435	0.55	0.06	52	3
IT58	Muttenz	264108	616912	Aalenian	Opalinus Ton	0.83	129	60	433	0.55	0.06	50	3
IT65	Muttenz	262950	617802	Aalenian	Opalinus Ton	0.43	75	24	431	[0.69]	0.13	40	3
EARLY JURASSIC													
IT7	Staffelegg	254000	647000	Toarcian	Jurensis Mergel	0.82	172	10	436	0.58	0.07	46	3
IT8	Staffelegg	254000	647000	Toarcian	Jurensis Mergel	0.78	169	12	436	[0.44]	0.11	26	3
IT30	Delémont	245223	581430	Toarcian	Jurensis Mergel	0.79*	240*	94*	429*	0.62	0.09	15	1
IT66	Muttenz	262950	617802	Toarcian	Jurensis Mergel	0.22	55	57	429	0.52	0.06	50	3
IT67	Muttenz	262950	617802	Toarcian	Jurensis Mergel	0.22	36	27	426	0.69	0.08	13	1
IT1	Schämbelen	257000	659000	Toarcian	Posidonia Schiefer	3.82	329	48	436	0.49	0.09	52	3
IT20	Delémont	245223	581430	Toarcian	Posidonia Schiefer	6.06*	711*	14*	427*	0.54	0.09	60	1
IT21	Delémont	245223	581430	Toarcian	Posidonia Schiefer	8.24*	720*	11*	428*	0.48	0.09	36	2
IT22	Delémont	248683	578875	Toarcian	Posidonia Schiefer	4.79*	668*	12*	425*	0.45	0.07	46	2
IT23	Delémont	248683	578875	Toarcian	Posidonia Schiefer	10.06*	742*	12*	426*	0.53	0.09	58	2
IT24	Delémont	248683	578875	Toarcian	Posidonia Schiefer	7.51*	695*	16*	428*	0.53	0.10	46	2
IT25	Delémont	248070	579180	Toarcian	Posidonia Schiefer	4.66*	790*	16*	427*	0.48	0.06	44	2
IT26	Delémont	248070	579180	Toarcian	Posidonia Schiefer	4.24*	710*	16*	424*	0.54	0.08	29	2
IT28	Delémont	245223	581430	Toarcian	Posidonia Schiefer	10.14*	693*	8*	424*	0.50	0.10	55	1
IT29	Delémont	245223	581430	Toarcian	Posidonia Schiefer	7.85*	663*	14*	429*	0.51	0.09	50	1
IT62	Muttenz	264222	616811	Sinemurian	Obtusus Ton	0.50	21	6	432	[0.63]	0.14	25	1
IT68	Muttenz	262950	617802	Sinemurian	Obtusus Ton	0.56	32	17	429	0.61	0.06	45	1
IT52	Frick	262000	642000	Hettangian	Insektenmergel	0.44	31	-	430	[0.66]	0.11	30	3
IT53	Frick	262000	642000	Hettangian	Insektenmergel	3.07	262	11	429	0.54	0.08	36	3
IT63	Muttenz	264222	616811	Hettangian	Insektenmergel					0.70	0.09	44	3
LATE TRIASSIC													
IT14	Grindel	247500	605000	Rhaetian	Rhät	0.68	69	81	434	0.80	0.06	70	3
IT31	Delémont	248070	579180	Rhaetian	Rhät					0.56	0.10	22	1
IT49	Balmberg	234800	608300	Rhaetian	Rhät					0.55	0.09	53	3
IT50	Delémont	248683	578875	Rhaetian	Rhät	0.61*	89*	18*	432*	0.61	0.10	76	3
IT51	Delémont	248683	578875	Rhaetian	Rhät	0.63*	47*	9*	427*	[0.65]	0.12	25	3
IT64	Muttenz	264222	616811	Rhaetian	Rhät	0.40	67	13	433	0.66	0.09	50	3
IT68a	Muttenz	262950	617802	Rhaetian	Rhät	0.50	101	37	435	0.49	0.08	20	1
IT37	Trimbach	247000	633500	Middle Keuper	Gipskeuper					[0.66]	0.13	55	3
IT38	Trimbach	247000	633500	Middle Keuper	Gipskeuper					[0.78]	0.15	74	1
IT39	Belchenflue	246300	628200	Middle Keuper	Gipskeuper					[0.75]	0.11	65	3
IT59	Muttenz	264299	616673	Middle Keuper	Gipskeuper					[0.64]	0.12	32	3
IT69	Muttenz	262765	617994	Middle Keuper	Gipskeuper	0.70	256	16	435	0.64	0.09	30	3
IT70	Muttenz	262765	617994	Middle Keuper	Gipskeuper	0.88	116	11	425				
IT60	Muttenz	264299	616673	Early Keuper	Letten Kohle	0.30	157	45	436	0.69	0.08	50	3
IT61	Muttenz	264299	616673	Early Keuper	Letten Kohle	0.28	60	18	431	[0.70]	0.13	52	3
MIDDLE TRIASSIC													
IT71	Muttenz	263832	617060	Late Muschelkalk	Trigonodus Dolomit	1.41	289	10	432	0.76	0.09	33	3

Table 1. Sample location and identification, Rock-Eval pyrolysis and vitrinite reflectance data. OSM = Upper Freshwater Molasse, OMM = Upper Marine Molasse, USM = Lower Freshwater Molasse, UMM = Lower Marine Molasse, TOC = total organic carbon (% weight); HI = hydrogen index (mg HC/g TOC); OI = oxygen index (mg CO_2/g TOC); Tmax = maximum pyrolysis temperature (°C); % Rr = mean random vitrinite reflectance, values in brackets should be treated with care as the standard deviations are too high (> 0.1); S = standard deviation; N = number of vitrinite reflectance measurements; PM = preparation method; (1) whole rock polished section, (2) polished organic section, (3) polished isolated kerogen section, (4) pellets of particulate phytoclasts; Rock-Eval pyrolysis data marked with a star are from Gorin & Feist-Burkhardt (1990).

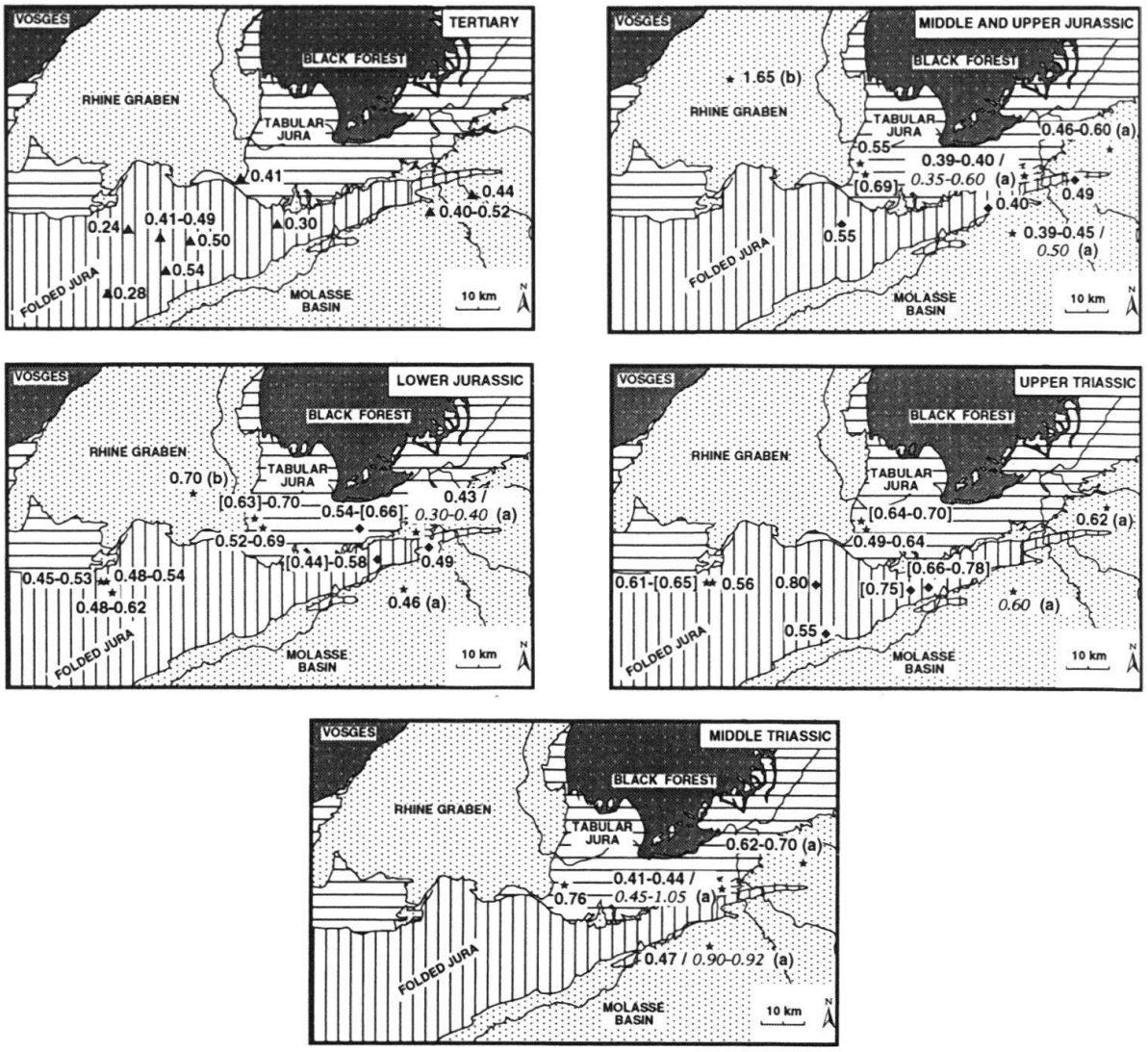

Fig. 3. Tectonic maps with mean random vitrinite reflectance values (% Rr) for Tertiary, Middle and Upper Jurassic, Lower Jurassic, Upper and Middle Triassic sediments. (a) data for the wells Weiach, Schafisheim and Riniken from Matter et al. (1988a), Matter et al. (1988b) and Matter et al. (1987) respectively; figures in italic are vitrinite reflectance values based on spectral fluorescence measurements; (b) data from Robert (1985). Vitrinite reflectance values in brackets should be treated with care as the standard deviations are too high (> 0.1).

4.2 Middle and Upper Jurassic

5 outcrop samples from 3 different formations (Effinger Schichten, Hauptrogenstein, Opalinus Ton) have been analysed. Vitrinite reflectance values range from 0.40% Rr for a sample of the Hauptrogenstein to 0.69% Rr for a sample of the Opalinus Ton. Our maturity determinations correlate with previous studies carried out in three deep wells of the NAGRA, situated in the eastern part of the study area (Matter et al. 1987, 1988a, 1988b). According to these authors, vitrinite reflectance values of Middle and Upper Jurassic sediments in these wells range from 0.39% Rr (Effinger Schichten, well Schafisheim) to 0.60% Rr (Opalinus Ton, well Weiach). The geographical distribution of the vitrinite reflectance data for the Middle and Upper Jurassic (Fig. 3) indicates an increase of maturity from south-east to north-west.

4.3 Lower Jurassic

20 samples from Lower Jurassic formations (Jurensis Mergel, Posidonia Schiefer, Obtusus Ton, Insektenmergel) have been studied. Some of the samples have been taken from shallow coreholes (Delémont, Muttenz), others from outcrops. The mean vitrinite reflectance varies between 0.44% Rr (Jurensis Mergel) and 0.70% Rr (Insektenmergel). These results are similar to those observed in the Middle und Upper Jurassic. Geographically, vitrinite reflectance values indicate an increase in maturity of Liassic sediments from SE to NW, towards the Rhine Graben (Fig. 3). This trend is not in accordance with a map published by Brink et al. (1992) showing a NW-SE increase of source rock maturity of shales of Toarcian age in Northern Switzerland. As the raw data for the construction were not published by these authors, the reasons for this discrepancy cannot be evaluated.

4.4 Middle and Upper Triassic

Vitrinite reflectance values of 1 Middle Triassic and 15 Upper Triassic samples from shallow coreholes (Muttenz and Delémont) and outcrops have been determined. The measured Rr values range between 0.49% Rr (Rhät) and 0.80% Rr (Rhät). Rr-histograms of Triassic samples show typically a big scatter of the reflectance measurements. This may be due to the presence of oxidised or reworked vitrinite. No systematic geographical variation of the vitrinite reflectance values could be observed (Fig. 3).

4.5 Vitrinite reflectance gradients

According to Wolf & Hagemann (1987, their Table 4) the increase of vitrinite reflectance with depth for the Mesozoic section in the NAGRA wells Schafisheim, Weiach and Riniken is 0.65, 0.37 and 0.96% Rr/km respectively. The reconstruction of 5 complete stratigraphic profiles based on information from outcrops, shallow boreholes and literature (more details in chapter 6.1 and Table 2) allowed to obtain roughly estimated reflectance gradients of Mesozoic and Tertiary sediments in the south of the Rhine Graben. The following values were calculated: Delémont 0.3% Rr/km, Muttenz 0.8% Rr/km, Trimbach 0.5% Rr/km, Passwang 0.5% Rr/km and Staffelegg 0.7% Rr/km.

5. Organic geochemistry

13 samples from Jurassic sediments and 8 from Triassic rocks in shallow boreholes and outcrops were analysed by Rock-Eval pyrolysis. The results are summarised in Table 1, and the diagram hydrogen index (HI) versus oxygen index (OI) indicating the type of kerogen is shown in Figure 4.

Samples from the Posidonia Schiefer consist of marine type I–II kerogen (Fig. 4). Most of the pyrolysis data for this formation (Table 1) are taken from the original file of Gorin & Feist-Burkhardt (1990). According to these authors, the Posidonia Schiefer is an oil prone source rock with a significant generation capacity (average TOC = 7.1% and average HI = 715 mg HC/g TOC). One sample (IT 1) taken from an outcrop has significantly lower TOC (3.82%) and HI (329 mg HC/g TOC) values. This is probably due to weathering, as stated by Espitalié et al. (1986) for similar cases.

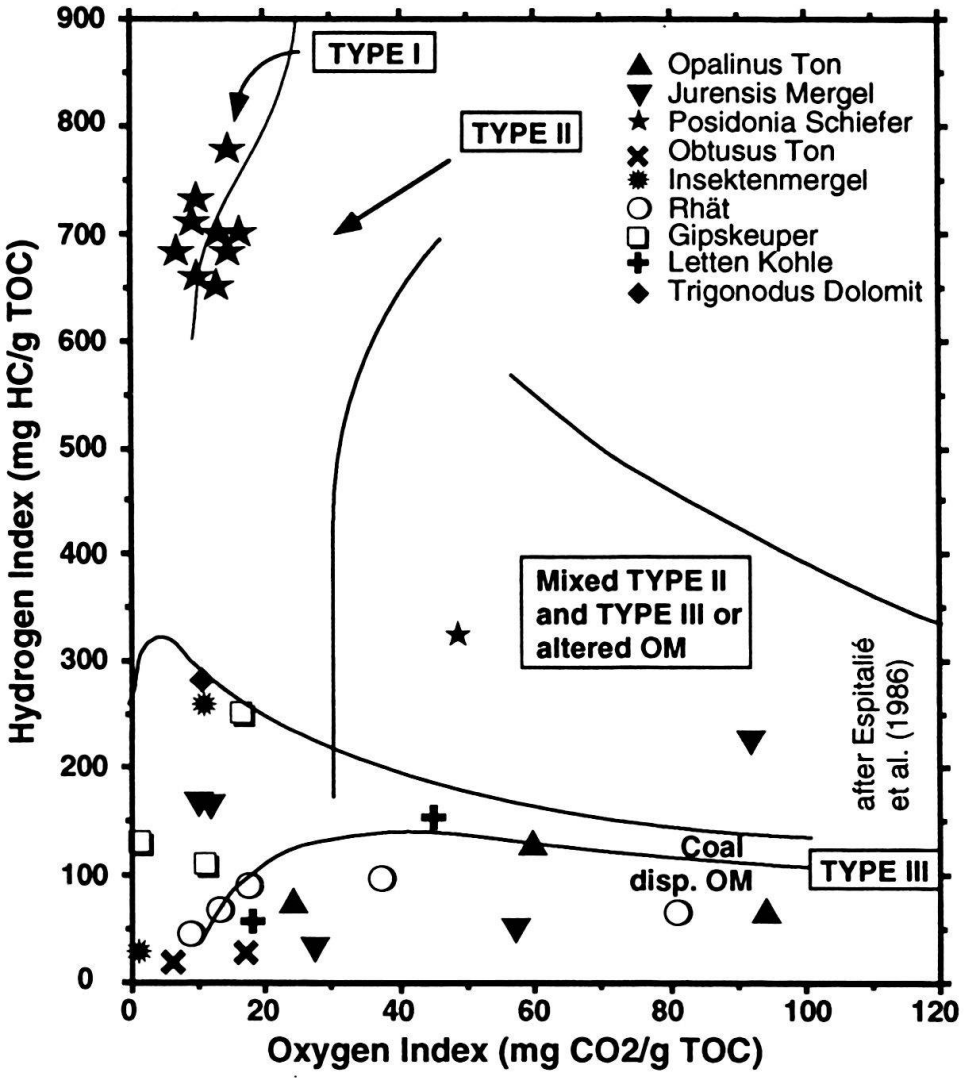

Fig. 4. Results of Rock-Eval pyrolysis based on Triassic and Jurassic sediments: HI (hydrogen index) versus OI (oxygen index) diagram. Note that samples from the Posidonia Schiefer consist of kerogen of type I–II. All other samples contain type III kerogen. Most data for the Posidonia Schiefer are from Gorin & Feist-Burkhardt (1990).

These results are supported by petrographical observations. The Posidonia Schiefer consist mainly of hydrogen-rich, strongly fluorescing organic constituents. A major part of the organic matter in this formation is absorbed and incorporated within the clay minerals forming the "mineral-bituminous groundmass" (a term involved by Teichmüller & Ottenjann 1977). Tasmanales alginites, yellow fluorescing liptodetrinites and different types of bituminites could be identified in the light brown fluorescing groundmass. Humodetrinites are relatively rare, rounded in form (humocorpocollinites) and inertinites occur primarily as inertodetrinite.

All other samples contain type III kerogen with low HI values. Petrographical observation of this second group shows a predominance of humodetrinite and inertodetrinite confirming the organic geochemistry results.

The HI versus Tmax diagram can be used to estimate roughly the thermal maturity (Espitalié et al. 1986). Our plots indicate (Fig. 5a and b) that most samples are at the

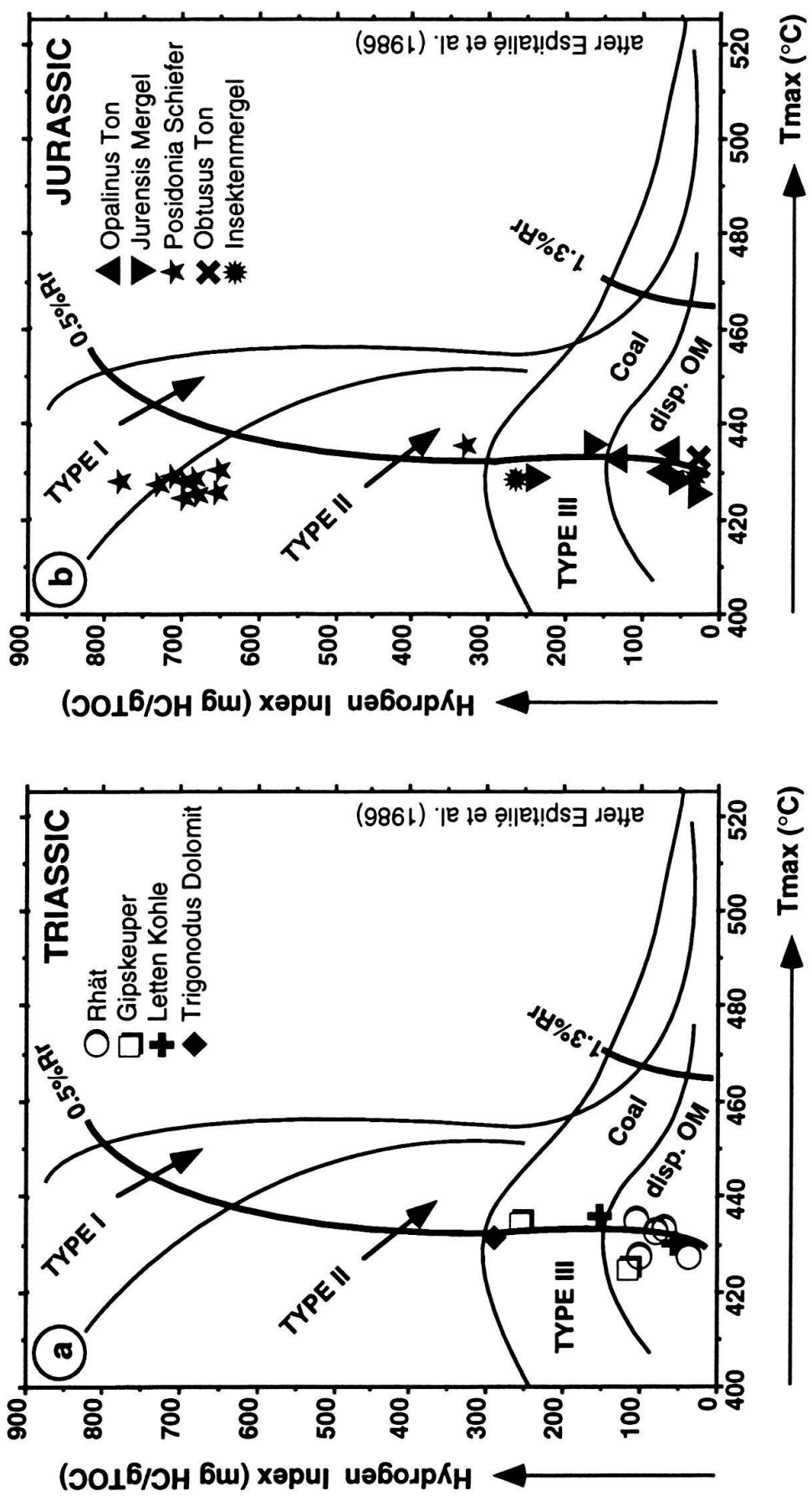

Fig. 5. Results of Rock-Eval pyrolysis based on a) Triassic and b) Jurassic sediments: HI (hydrogen index) versus Tmax (maximum pyrolysis temperature). Note that samples are at the onset of the oil generation zone. Most data for the Posidonia Schiefer are from Gorin & Feist-Burkhardt (1990).

onset of the oil generation zone, which may start at vitrinite reflectance values between 0.5 and 0.7% Rr (Tissot & Welte 1984). The correlation of Tmax with Rr resulted in an insignificant positive relationship ($r^2 = 0.37$). This may be due to the fact that Tmax is a crude measurement of thermal maturity and is partly dependent on other parameters, such as the type of kerogen.

6. Thermal modelling

6.1 Model algorithm and evaluation of the parameters

The vitrinite reflectance of source rocks and coals is a widely used indicator of organic maturity (Stach et al. 1982; Tissot et al. 1987) and has become a standard parameter for quantifying the sediment diagenesis (Bustin et al. 1985). An important tool for the interpretation of maturity results is thermal modelling which is considered to be an integrated part of basin analysis (Welte & Yalçin 1988). Most of these models use burial diagrams and a "known" temperature history in order to predict the maturation levels of a stratigraphic succession (Lopatin 1971; Bostick 1974; Hood et al. 1975; Waples 1980; Lerche et al. 1984). We used one of the recently developed kinetic models (EASY% Ro, Sweeney & Burnham 1990) for the calculation of the vitrinite reflectance evolution.

Our approach for modelling the thermal maturation levels of Mesozoic and Cenozoic rocks in the study area is similar to the one described by Todorov et al. (1992):

i) Construction of burial history diagrams

The Mesozoic and Tertiary burial histories of 8 sites (see Table 2 and Fig. 2 for location) in Northern Switzerland have been constructed. A review of subsidence history analysis in the context of the Swiss Plateau and the Jura is given in Wildi et al. (1989) and Loup (1992b). The subsidence curves have been constructed with BACKSTRIP89 (for a description see Loup 1992a). This basin analysis program takes into account parameters such as sediment thickness (present day thickness, compaction, erosion and deformation), age of sediments, depositional depth and eustatic sea-level variations. For thermal modelling, however, only simple burial diagrams (without eustatic and bathymetric corrections) have been used.

The input data for the calculation of subsidence curves were taken from literature, such as geological maps, explanation notes to geological maps and regional or thematic publications:

- Delémont: Liniger (1925), Suter (1978), Naef et al. (1985), Mont Terry section after Wildi et al. (1989)
- Muttenz: Geologische Karte Arlesheim (Blatt 1067, 1:25000) mit Erläuterungen, Naef et al. (1985)
- Trimbach: Geologische Spezialkarte 73, Mühlberg/Hauensteingebiet (1:25000) mit Erläuterungen, Müller et al. (1984), Naef et al. (1985), Diebold et al. (1991)
- Passwang: Naef et al. (1985), Wildi et al. (1989)
- Staffelegg: Geologische Spezialkarte 45, Mühlberg/Aarau (1:25000), Müller et al. (1984), Naef et al. (1985), Diebold et al. (1991)
- Weiach: Naef et al. (1985), Matter et al. (1988a), Nagra (1988), Diebold et al. (1991)
- Schafisheim: Naef et al. (1985), Matter et al. (1988b), Nagra (1988), Keller et al. (1990), Diebold et al. (1991)
- Riniken: Naef et al. (1985), Matter et al. (1987), Diebold et al. (1991)

It has long been realised that the rank of coal is mainly a function of time and temperature (Karweil 1956). Some recent publications suggested, however, that the effect of the duration of heating on thermal maturation of organic matter is limited (Barker 1983, 1989, 1991; Price 1983, Suggate 1982). According to these authors, the thermal maturity of organic matter seems to be mainly determined by the attained maximum paleotemperatures. A crucial point of our approach is, therefore, the estimate of the maximum paleodepth which corresponds most probably also to the temperature climax.

The Triassic-Early Cretaceous subsidence history of Western and Central Europe was governed by intra-plate tensional stresses (Loup 1992, cum biblio) which were related to the break-up of Pangea (Ziegler 1987). Western and Central Europe became progressively subjected to regional extension resulting in the development of a complex, multidirectional system of grabens and troughs, many of which are superimposed on Late Paleozoic fracture systems (Ziegler 1988).

During Triassic to Middle Jurassic, the study area was a part of the intracontinental German Basin. The so-called "Vindelician High" (extending south-westwards from the Bohemian Massif) separated the German Basin from the broad shelf of the Tethys in the south (Trümpy 1980, Bachmann et al. 1987). This basement high was gradually overstepped from NW to SE by Triassic to Jurassic sediments up to 1000 m thick. The thickness of Triassic and Jurassic strata in the study area is smaller due to the NW-striking Zurich High which became apparent for the first time during the Late Triassic (Bachmann et al. 1987).

Fairly high subsidence rates during Middle and Late Triassic are observed in the Jura (Wildi et al. 1989). Subsidence rates are abruptly diminishing during the Early Jurassic and are accelerating again in an irregular pattern in the Middle Jurassic. The Triassic and Middle Jurassic phases are probably due to intracontinental rifting following Late Variscan structures (Wildi et al. 1989).

During the Late Jurassic (Malm) the Vindelician High became fully inundated and up to 600 m of limestones and marlstones were deposited. Unlike the Triassic to Middle Jurassic series, the Malm thickens towards the SE rather than the N or NW, emphasising, therefore, the integration of the future Molasse basin into the Tethys shelf (Bachmann et al. 1987).

No sediments of Cretaceous age are found in the study area. Tertiary strata lie unconformably on Upper Jurassic sediments. This sedimentary gap is, at least in part, due to the latest Cretaceous-earliest Tertiary inversion tectonics which can be related to stresses that were exerted by the Alpine and Pyrenean orogenic events on the continental forelands of these foldbelts (Ziegler 1987, 1992). The uplift of large areas in the German Molasse basin resulted in a north-westward truncation of Cretaceous and Upper Jurassic strata (Bachmann & Müller 1991). In the Swiss Molasse basin and the Jura, Cretaceous sediments are only found in the western part of the country (Lemcke 1974, Wildi et al. 1989), whereas in the eastern part, in the area of the Zurich High (extending from Northeast Switzerland to the southern Rhine valley), Mesozoic strata were eroded down to the Oxfordian (Bachmann & Müller 1991). It is, however, uncertain to what extent the area occupied by the Rhine Graben and the South German Franconian Platform may have been covered by Cretaceous seas (Ziegler 1988). According to Lemcke (1988) this area was a region with little or no sediment accumulation throughout the Cretaceous.

There are other observations indicating that Cretaceous strata have never been very thick in our study area:

- The thickness of Lower Cretaceous strata (up to Cenomanian) in sections of the Jura, lying just west of the study region, rarely exeeds 100 m (sections Maiche, Montbéliard or Besançon in Wildi et al. 1989).
- The Cretaceous transgression advanced from the Helvetic shelf area in the south, and Cretaceous strata become thinner and more uncomplete towards the north (Trümpy 1980, Bachmann & Müller 1991, their figs. 20.4 & 20.5).
- According to Wildi et al. (1989), the subsidence of the Helvetic margin due to passive continental margin evolution is almost terminated at the end of the Late Jurassic. The Cretaceous subsidence history is probably already controlled by orogenic crustal flexure, with high subsidence rates only in the southernmost parts of the Helvetic realm (sections Aravis, Aermighorn & Alvier in Wildi et al. 1989).

For the reconstruction of the subsidence history we assumed, therefore, a thickness of Early Cretaceous strata of only 100 m. These deposits are supposed to be eroded during the Late Cretaceous-Early Tertiary inversion phase.

A phase of rapid subsidence which started in Oligocene and ended in Late Miocene with the beginning of the Jura folding (Naef et al. 1985) terminated the deposition history in the study area. The subsidence pattern is mainly controlled by the Rhine Graben rifting (especially for areas in the southern prolongation of the Rhine Graben) and the tectonic loading of the European lithosphere by the Alpine nappes. The amount of the burial and subsequent uplift/erosion in the study area is a badly defined value.

A recent study on rock density and compaction postulates Neogene erosion values of up to 4 km for the deep wells of Schafisheim and Weiach (Kälin et al. 1992). Brink et al. (1992), based on porosity and velocity evaluations in Middle Jurassic rocks, assumed post-Jurassic uplift values of up to 2500 m in our study area. There is, however, no geological evidence for such large amounts of burial and consecutive uplift/erosion in the distal parts of the Molasse basin (Laubscher 1974, Lemcke 1974, Schegg 1992b, 1993). Proposed maximum erosion estimates for the western part of the Molasse basin, where the youngest strata of the Molasse sequence are missing (contrary to Eastern Switzerland), are in the order of only 1–2 km (Monnier 1982, Schaer 1992). Another argument against deep burial in the outer part of the foreland basin is the formation of the foreland bulge, due to the flexural response of the lithosphere on thrust loading at the Alpine front (Sinclair et al. 1991). According to Laubscher (1992), the two important Neogene erosional events, at the external flank of the Molasse basin (see Naef et al. 1985), may be considered candidates for an approximate location of the formation of the foreland bulges corresponding to the two Neoalpine phases.

Our burial history reconstruction for the Neogene is mainly based on observed and regionally extrapolated sediment thicknesses in the distal part of the Molasse basin (see references in section 6.1.i). The chosen values for burial and subsequent uplift/erosion are probably minimal estimates and paleogeothermal gradients resulting from our calculations are consequently maximal estimates.

ii) Construction of a time-temperature history

The burial diagrams combined with an initial set of paleogeothermal gradients and mean annual surface temperatures enable the calculation of a time-temperature history for each formation. Generally, several thermal histories may result in the same maturation profile. Therefore, it is essential in thermal modelling to begin with an evaluation of the tectonic history of the study area in order to reveal its thermal implications (see chapter 6.1.i). This preliminary examination should lead to a reliable initial set of paleogeothermal parameters.

The oldest, stratigraphically documented tectonic event of Northern Switzerland is the late Paleozoic development of local transtensional and pullapart basins accompanied by a widespread volcanism (Ziegler 1988). Thermal modelling of the borehole Weiach by Kempter (1987) suggests paleogeothermal gradients of about 104 °C/km until the end of the Early Permian.

According to Ziegler (1988), the Triassic and Middle Jurassic intraplate rifting phases in Western and Central Europe were accompanied by only very minor volcanic activity. The author concluded that the subsidence phases were due to regional crustal extension rather than to the development of a multitude of local hotspots or mantle plumes. In our temperature modelling, we therefore, assume a "normal" paleogeothermal gradient of 30 °C/km for the Triassic, Jurassic and Lower Cretaceous.

About 100 my. ago, volcanic activity set in, widespread over the future Rhine Graben and its shoulders, but concentrated on its main fracture zones (Baranyi et al. 1976, Illies 1977). The volcanic activity preceding the Eocene rifting process of the Rhine Graben demonstrates the mantle upwelling evolved since mid-Cretaceous times (Illies 1977), and indicates increased paleogeothermal gradients in the Rhine Graben area. We assume a gradient of 50 °C/km for this pre-rifting period.

The major tectonic events in the study area (Rhine Graben rifting and Jura folding) took place between Late Eocene and late Middle Miocene (Laubscher 1982). The thermal history of the Rhine Graben is characterised by a major phase of geothermal flux in the Eocene, preceding somewhat the main rifting process which started in Middle Eocene times (Teichmüller & Teichmüller 1979, Robert 1985). Teichmüller & Teichmüller (1979) reported paleogeothermal gradients in the middle Upper Rhine Graben reaching values of up to 80 °C/km. During the Oligocene period, the two main graben fillings, the Sannoisian and the Rupelian sediments, were thickest in the Alsass area; correlatively, the evolution of the organic matter reveals a concomitant hyperthermy (Robert 1985). No sediments of Miocene age are preserved in the southern part of the Rhine Graben (Illies 1977). Paleogeothermal reconstructions (Buntebarth 1979, Teichmüller & Teichmüller 1979) in the northern part indicate that geothermal gradients decreased to values < 50 °C/km during this period. According to Laubscher (1992), in post-Early Miocene times, the southern part of the Rhine Graben became the locus of "constructive interference" with the Alpine forebulge. This new stress system resulted in the uplift of the Rhine dome (Black Forest-Vosges). The dome was supported by hot asthenospheric masses supplanting part of the lithosphere and somehow provoking crustal thinning (Werner & Kahle 1980, Laubscher 1992). The resulting geothermal conditions are indicated by the increased volcanic activity (Kaiserstuhl, Hegau) in the southern parts of the Rhine Graben realm. Indications for a high temperature regime south of the Rhine Graben

realm are given by Mullis (1987). According to this author a group of salt-poor fluid inclusions from the NAGRA deep well Schafisheim in northern Switzerland was most probably trapped during the Jura folding (Middle to Late Miocene) at temperatures between 70 and 140 °C. The calculated paleogeothermal gradients for the well Schafisheim are between 50 and 60 °C/km.

For our modelling approach we assumed that a high paleogeothermal regime in the study area prevailed between Late Eocene and Late Miocene. We also postulate that the paleogeothermal gradients at the end of the Cenozoic have been close to the present ones (Rybach et al. 1987).

The mean annual temperature at the sediment/air or at the sediment/water interface was estimated at 15 °C during the Mesozoic and Tertiary. Palynological investigations (Hochuli 1978) suggest, for example, temperatures of 15–18 °C for the North Alpine Foreland during the Oligocene. Present day values are set at 10 °C.

iii) Simulation of the vitrinite reflectance evolution

The time-temperature histories of different formations of a stratigraphic section are then introduced into the EASY % Ro model of Sweeney & Burnham (1990) in order to calculate its maturation profile.

iv) Calibration of modelling results

Comparison between modelled and measured vitrinite reflectance enables the optimisation of the paleogeothermal model: the thermal constraints (in our cas the geothermal gradient during the Tertiary) are changed until there is a fit between modelled and measured values.

This approach will not result in a unique solution, because several thermal histories may lead to the same maturation profile. Moreover, admitting uncertainties of the input parameters, it is obvious that our calculations cannot be more than a first approximation which has to be calibrated with other methods.

6.2 Thermal modelling results

The thermal histories of 8 sections comprising Cenozoic and Mesozoic sediments have been modelled (see results summarised in Table 2). The vitrinite reflectance evolution for five formations of the profile Muttenz and the correlation between measured and calculated values are shown in Figure 6. Maturation histories for the oldest formations of the 8 studied profiles are represented in Figure 7.

As burial diagrams indicate, maximum paleodepth were attained during the Late Miocene (Fig. 7). For the oldest modelled formations of each profile, these depths range between 860 m (Staffelegg, Insektenmergel) and 1990 m (Schafisheim, Orbicularis Mergel).

The calculated maximum paleotemperatures for the different formations are as follows: Middle Triassic formations (77–127 °C), Upper Triassic formations (88–119 °C), Lower Jurassic formations (65–106 °C), Middle Jurassic formations (53–104 °C), Upper Jurassic formations (72 °C) and Tertiary formations (26–70 °C). With the

					Thermal Modelling		
Modelled Profile	Location	Formation	Age	%Rr - measured	%Rr- calculated	Tmax (°C)	PGG (°C/km)
DELEMONT	Delémont	Rhät	Late Triassic	0.56-[0.65]	0.59	97	80
	Delémont	Jurensis Mergel	Early Jurassic	0.62	0.58	96	
	Delémont	Posidonia Schiefer	Early Jurassic	0.45-0.54	0.58	96	
	Delémont	UMM s.l.	Oligocene	0.49	0.29	37	
	Delémont	Molasse alsacienne	Oligocene	0.41	0.28	36	
	Tramelan	OSM	Miocene	0.28	0.26	26	
	Bois de Raube	Vogesenschotter	Miocene	0.24	0.26	26	
MUTTENZ	Muttenz	Trigonodus Dolomit	Middle Triassic	0.76	0.71	123	100
	Muttenz	Letten Kohle	Late Triassic	0.69-[0.70]	0.68	119	
	Muttenz	Gipskeuper	Late Triassic	[0.64]	0.66	117	
	Muttenz	Rhät	Late Triassic	0.49-0.66	0.62	108	
	Muttenz	Insektenmergel	Early Jurassic	0.70	0.60	106	
	Muttenz	Obtusus Ton	Early Jurassic	0.61-[0.63]	0.59	104	
	Muttenz	Jurensis Mergel	Early Jurassic	0.52-0.69	0.57	102	
	Muttenz	Opalinus Ton	Middle Jurassic	0.55-[0.69]	0.56	101	
TRIMBACH	Belchenflue and Trimbach	Gipskeuper	Late Triassic	[0.66-0.78]	0.67	111	50
	Brocheni Flue	USM	Oligocene	0.30	0.41	70	
PASS-WANG	Balmberg and Grindel	Rhät	Late Triassic	0.55-0.80	0.57	94	70
	Meltingen	Opalinus Ton	Middle Jurassic	0.55	0.55	92	
	Brocheni Flue	USM	Oligocene	0.30	0.32	45	
STAFFEL-EGG	Frick	Insektenmergel	Early Jurassic	0.54-[0.66]	0.51	88	85
	Staffelegg	Jurensis Mergel	Early Jurassic	[0.44]-0.58	0.50	85	
	Schämbelen	Posidonia Schiefer	Early Jurassic	0.49	0.50	85	
	Asperchlus	Hauptrogenstein	Middle Jurassic	0.40	0.42	71	
WEIACH	Well Weiach	Wellen Mergel	Middle Triassic	0.70*	0.75	127	75
		Orbicularis Mergel	Middle Triassic	0.62*	0.74	125	
		Letten Kohle	Late Triassic	0.62*	0.67	116	
		Opalinus Ton	Middle Jurassic	0.60*	0.60	104	
		Würtenbergia Schichten	Middle Jurassic	0.55*	0.52	93	
		Küssaburg Schichten	Late Jurassic	0.46*	0.45	83	
SCHAFIS-HEIM	Well Schafisheim	Orbicularis Mergel	Middle Triassic	0.47 / 0.90-0.92 (f)**	0.55	95	40
		Estherien Schiefer	Late Triassic	0.60 (f)**	0.51	88	
		Insektenmergel	Early Jurassic	0.46**	0.48	83	
		Opalinus Ton	Middle Jurassic	0.50 (f)**	0.47	82	
		Blagdeni Schichten	Middle Jurassic	0.45**	0.45	78	
		Effinger Schichten	Late Jurassic	0.39**	0.42	72	
	Mägenwil	OMM	Miocene	0.48	0.29	36	
	Hanenberg	OMM	Miocene	0.40	0.29	36	
RINIKEN	Well Riniken	Orbicularis Mergel	Middle Triassic	0.41 / 0.80-1.05 (f)***	0.47	82	60
		Dolomitmergel	Middle Triassic	0.44 / 0.45-0.50 (f)***	0.47	81	
		Trigonodus Dolomit	Middle Triassic	0.55-0.65 (f)***	0.44	77	
		Posidonia Schiefer	Early Jurassic	0.43 / 0.30-0.40 (f)***	0.39	65	
		Opalinus Ton	Middle Jurassic	0.35-0.60 (f)***	0.38	63	
		Hauptrogenstein	Middle Jurassic	0.40 / 0.40 (f)***	0.34	53	

Table 2. Thermal modelling of 8 sections of the study area (for explanation see chapter 6 and fig. 7): % Rr = mean random vitrinite relfectance; values in brackets should be treated with care as the standard deviations are too high (> 0.1); Tmax = calculated maximum palaeotemperature for each modeled formation; PGG = calculated paleogeothermal gradients during Late Paleogene and Early Neogene; (*), (**) and (***): vitrinite reflectance values from Matter et al. (1988 a), Matter et al. (1988 b) and Matter et al. (1987) respectively; vitrinite reflectance values marked by (f) are based on spectral fluorescence mesurements.

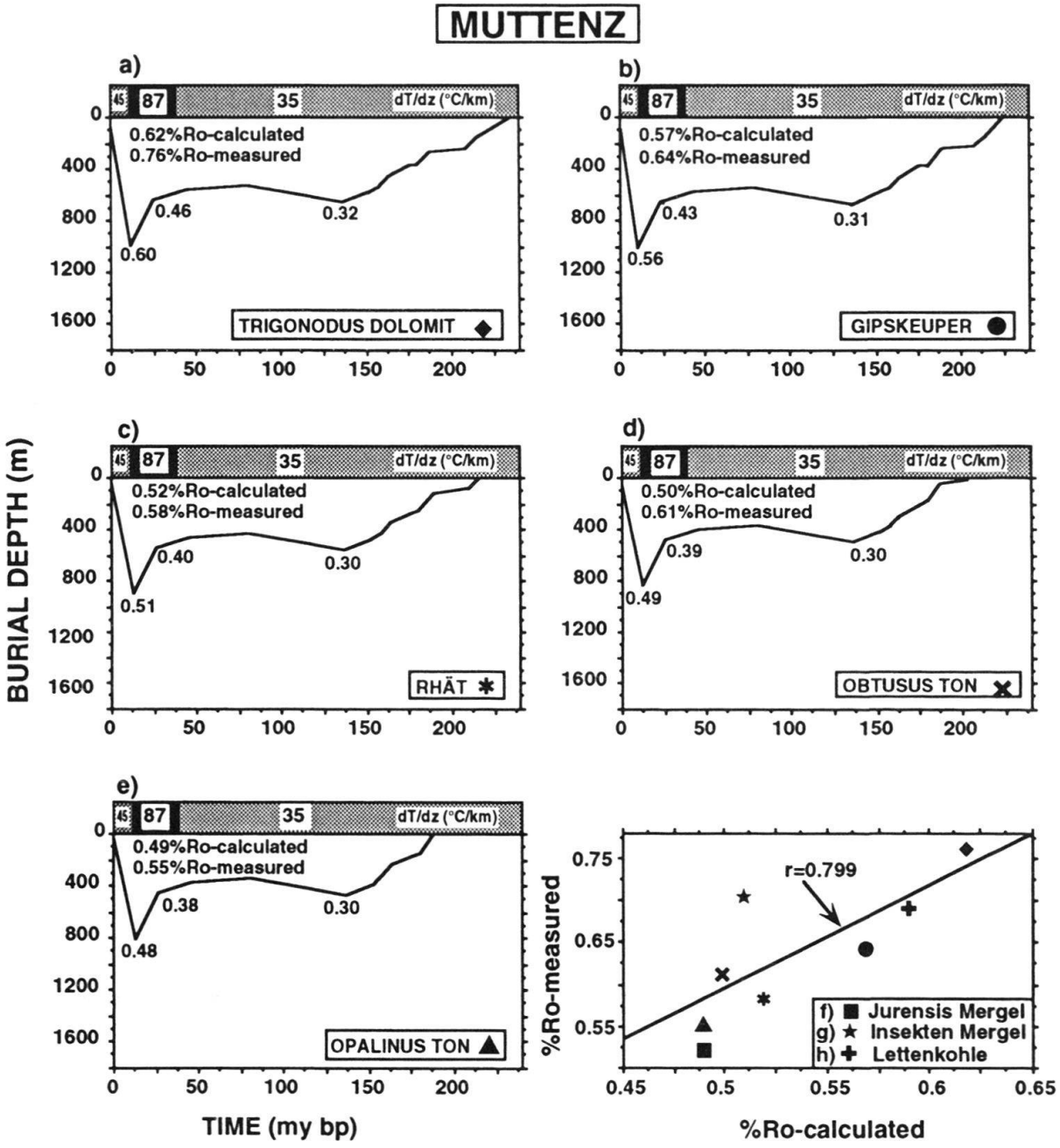

Fig. 6. Thermal modelling of the Muttenz section: calculated Rr values for different formations are indicated during burial history [burial depth (m) versus age before present (my bp)]. For the present (0 my bp) the calculated and the measured values are shown. Vitrinite reflectance values in brackets should be treated with care as the standard deviations are too high (> 0.1). Variations of the geothermal gradients (dt/dz) are shown in the heading of each burial history diagram. The diagram in the lower right corner shows the correlation of measured and calculated Rr values.

exception of the sections Schafisheim (40 °C/km) and Trimbach (50 °C/km), the corresponding paleogeothermal gradients during Late Eocene to late Middle Miocene are very high (60–100 °C/km).

Sections which are near the Rhine Graben (Muttenz and Delémont) or which are in the axes of the Permo-Carboniferous trough display high paleogeothermal gradients

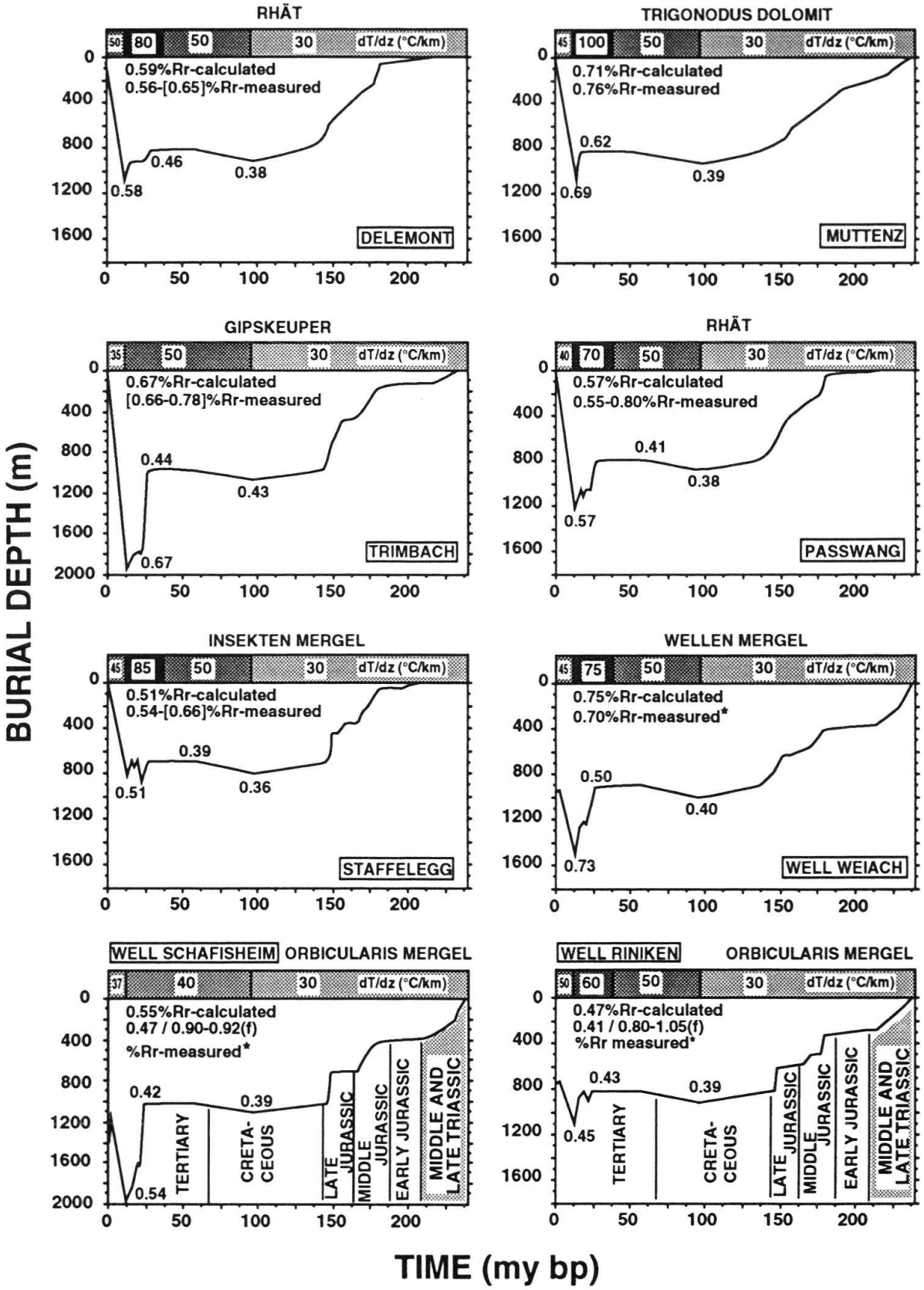

Fig. 7. Thermal modelling of the oldest sampled sedimentary formation in 8 stratigraphic sections (see Fig. 6 for explanation of the diagram). Measured Rr values marked with a star are from Wolf & Hagemann (1987); vitrinite reflectance values marked by (f) are based on spectral fluorescence measurements. Vitrinite reflectance values in brackets should be treated with care as the standard deviations are too high (> 0.1).

during Late Eocene to late Middle Miocene (60–100 °C/km), whereas sections, situated towards the Molasse basin (s.s.), show lower gradients (Trimbach and Schafisheim, 50 and 40 °C/km respectively).

Our results indicate that, due to a high paleogeothermal regime and an important burial depth, maturation of Mesozoic and Cenozoic sediments was completed only by the end of late Middle Miocene (Fig. 6 and 7). According to our model, the diagenesis level of the rocks rapidly increased during Late Oligocene to Late Miocene times. This hypothesis is also supported by the fact that the thermal maturity of Mesozoic sediments does not increase, even when modelling with a Mesozoic paleogeothermal gradient which is much higher than the assumed value of 30 °C/km.

7. Discussion and conclusion

The information resulting from the present investigations (vitrinite reflectance, organic geochemistry and thermal modelling) in the south of the Rhine Graben and the Eastern Jura can be summarised as follows:

i) Vitrinite reflectance values of Tertiary samples in the study area display a large range of values (0.24–0.54% Rr). The degree of diagenesis varies geographically. Relativley high vitrinite reflectance values are observed in the southern prolongation of the eastern Rhine Graben border.

ii) The measured vitrinite reflectance of Mesozoic sediments varies between 0.40 and 0.80% Rr. Vitrinite reflectance values of Jurassic sediments increase slightly from south-west to north-east, whereas Triassic samples show no geographical variation.

iii) The coalification gradients in the study area are high (0.3–0.96% Rr/km).

iv) The organic geochemistry analysis reveals the existence of two distinct groups of samples. Those from the Posidonia Schiefer are characterised by kerogen type I and II; all other sample from Mesozoic sediments contain type III kerogen. Tmax values from Rock-Eval pyrolysis confirm the maturity level established by vitrinite reflectance measurements.

v) Thermal modelling results indicate that the final (present-day) maturation level of the Mesozoic and Tertiary sediments was completed during Late Oligocene to Late Miocene. The inferred paleogeothermal gradients during this period are high (40–100 °C/km).

Thermal modelling has shown that very high paleogeothermal gradients during the Tertiary are necessary to explain the maturation level of Mesozoic and Tertiary sediments. There are, however, other indications for a Tertiary high geothermal regime in or near the study area:

- Coalification gradients, similar to those observed in the study area, are reported from the Rhine Graben by Teichmüller (1979). According to this author, coalification gradients and present day geothermal gradients in deep wells of the Upper Rhine Graben are quite high, ranging between 0.29 to 1.14% Rr/km and between 47.6 to 76.9 °C/km respectively. Generally, it is assumed that the higher the coalification gradient, the higher the paleogeothermal gradient (Bustin et al. 1985). The observed coalification gradients in the Rhine Graben and in the study area are an order of

magnitude higher than those of the Molasse basin, where the inferred Tertiary geothermal gradients vary between 20 and 30 °C/km (Rybach 1984, Teichmüller & Teichmüler 1986). For these reasons paleogeothermal gradients in the study area should be much higher than those of the Molasse basin. For the Rhine Graben, paleogeothermal gradients of up to 80 °C/km during the main rifting phases were proposed (Buntebarth 1979, Teichmüller & Teichmüller 1979). These values are close to those obtained by thermal modelling in this study. Given the uncertainties (e.g. erosion estimates) in our calculations, it seems that the paleogeothermal regime in both regions was quite similar during the Tertiary.

- A Tertiary high-temperature regime in Northern Switzerland is also indicated by a fluid inclusion study of Mullis (1987).

The inferred Tertiary high temperature regime in the study area could be due to an increased heat flow in the sequel of the Rhine Graben rifting and of the "constructive interference" of the Rhine Graben with the Alpine forebulge during post-Early Miocene times (Laubscher 1992). The Upper Rhine Graben is characterised by high present-day heat flow densities, going up to values of 160 mW/m^2 (Cermák 1979). A mean value of 112 $\pm$ 34 mW/m^2 was reported by Morgan (1982). Doebl et al. (1974) and Buntebarth (1979) found that the Rhine Graben was already an area of high heat flow during the peak volanic activity and early rift genesis during Early Tertiary. Generally, it seems that regions with high surface heat flow values are characterised by a weakened (e.g. thinned) continental crust (Cermák 1979). Indeed, the present-day heat flow anomaly in the Rhine Graben corresponds well with the mantle bulge underneath the rift (Illies 1975). According to this author the crust-mantle boundary is located at a depth of only 24 km below the Kaiserstuhl area. But the anomalous heat flow is not limited to the Rhine Graben structure itself; increased geothermal activity may be traced far to the NNE into the Braunschweig-Altmark region (Bram 1979).

A prolongation of the geothermal anomaly in the Rhine Graben into the study area is supported by the survey of heat flow densities (Bodmer 1982, Bodmer & Rybach 1984) and geothermal gradients (Rybach et al. 1987). The relatively high regional heat flow values may partly be explained by the reduced crustal thickness in the study area ranging from about 27 km in the northern part to about 33 km in the southern part (Illies 1975, Deichmann 1990). But as stated by Person & Garven (1992) even the estimates of lithosphere thinning in the Rhine Graben (s.s.) are too small to account for the observed present-day thermal anomalies. An additional heat transport by convection along fault zones is, therefore, probable (Meier et al. 1979). There is growing evidence that the paleogeothermal regime of sedimentary basins depends often directly upon the paleogeohydrological conditions (Oliver 1986, Beck et al. 1989, Person & Graven 1992, Schegg 1992a, 1992b, 1993). Geothermal anomalies are often caused by uprising deep groundwater or other fluids, including water from the basement along highly permeable zones (Hitchon 1984, Nesbitt 1990).

The geothermal regime in Northern Switzerland is characterised by a strong positive heat flow anomaly (> 150 mW/m^2) in the lower Aare valley which is associated directly with the southern margin of the Permocarboniferous trough at the main Jura overthrust (Griesser & Rybach 1989). According to these authors, uprising deep groundwater is favoured as the mechanism creating the observed anomaly. Their results reveal the

draining effect of the Permocarboniferous trough and indicate that vertical permeability is present in the vicinity of the trough even at depths of several kilometres. Previous diagenesis studies in the same region interpreted the presence of salt-poor fluids in the Triassic rocks as a result of enhanced groundwater activity already during the Tertiary (Mullis 1987, Ramseyer 1987).

The thermal maturity of Mesozoic and Cenozoic sediments may, therefore, be due to an enhanced convective heat supply in the study area between late Eocene and late Miocene. It is obvious that the distribution and the depth-range of deep faults, linear fractures and graben structures have strongly controlled the paleogeothermal pattern. The high density of faults in the study area active in Tertiary times supports this hypothesis. Numerous narrow grabens, normal faults and left-lateral strike-slip faults extend SSW-wards from the Rhine Graben into the Epivariscan Mesozoic cover of the Tabular Jura and into the folds and thrusts of the Folded Jura (e.g. Laubscher 1982, 1986, 1987). According to the same author (1987), even Palaeozoic fault zones were reactivated during Late Eocene and Early Miocene. The maturity pattern of Tertiary sediments (high vitrinite reflectance values in the prolongation of the eastern Rhine Graben border where tectonic fault activity is maximal, see figure 3a) is a further argument in favour of an enhanced regional heat flow due to convective heat transport along highly fractured zones.

Acknowledgements

We are indebted to S. Feist-Burkhardt, G. Gorin, M. Weidmann and the Geological Museum of Lausanne for providing samples. The Swiss Federal Railways and L. Hauber authorised sampling of Rail 2000 cores of Muttenz. We wish to thank also M. Floquet and F. Gischig for the preparation of the samples. We are indebted to the Institut Français du Pétrole (IFP) for performing the Rock-Eval analyses. For helpful discussions or critical review of the manuscript we would like to thank the following: G. Gorin, E. H. K. Kempter, W. Leu, B. Loup, J. Metzger and B. Ujetz. This research was granted by the Swiss national foundation for scientific research, and the Katzarovi foundation (Geneva). Reviews by R. Ferreiro Mählmann and B. Kübler helped to improve the manuscript.

REFERENCES

Bachmann, G. H., Müller, M. & Weggen, K. 1987: Evolution of the Molasse Basin (Germany, Switzerland). Tectonophysics 137, 77–92.

Bachmann, G. H. & Müller, M. 1991: The Molasse basin, Germany: evolution of a classical petroliferous foreland basin. In: Generation, accumulation, and production of Europe's hydrocarbons (Ed. by A. M. Spencer). Spec. Publ. Europ. Assoc. Petroleum Geoscientists No. 1, Oxford University Press, Oxford, 263–276.

Baranyi, I., Lippolt, H. J. & Todt, W. 1976: K-Ar Altersbestimmungen an Tertiären Vulkaniten des Oberrheingraben-Gebietes: II Die Alterstraverse vom Hegau nach Lothringen. Oberrh. geol. Abh. 25, 41–62.

Barker, C. E. 1983: Influence of time on metamorphism of sedimentary organic matter in liquid-dominated geothermal systems, western North America. Geology 11, 384–388.

– 1989: Temperature and time in the thermal maturation of sedimentary organic matter. In: Thermal histories of sedimentary basins: methods and case histories (Ed. by N. D. Naeser &. T. H. McCulloh). Springer-Verlag, New York, Berlin, Heidelberg, London, Paris, Tokyo, 73–98.

– 1991: Implications for organic maturation studies of evidence for a geologically rapid increase and stabilization of vitrinite reflectance at peak temperature: Cerro Prieto geothermal system, Mexico. Bull. amer. Assoc. Petroleum Geol. 75, 1852–1863.

Barker, C. E. & Pawlewicz, M. J. 1986: Concentration of dispersed organic matter for vitrinite reflectance analysis using a simple crush and float method. Soc. org. Petrol. Newsletter 3/3, 3.

BECK, A. E., GARVEN, G. & STEGENA, L. 1989: Hydrogeological regimes and their subsurface thermal effects. Geophysical Monograph 47, IUGG Vol. 2, Washington.

BODMER, PH. 1982: Geothermische Karte der Schweiz: Wärmestromdichte. Schweiz. Geophysikal. Komm., Wabern.

BODMER, PH. & RYBACH, L. 1984: Geothermal map of Switzerland (Heat flow density). Matér. Géol. Suisse, Sér. géophys. 22, Berne.

BOSTICK, N. H. 1974: Phytoclasts as indicators of thermal metamorphism, Franciscan Assemblage and Great Valley Sequence (Upper Mesozoic), California. Spec. Pap. geol. Soc. Amer. 153, 1–17.

BRAM, K. 1979: Heat flow measurements in the Federal Republic of Germany. In: Terrestrial heat flow in Europe (Ed. by V. CERMÁK & L. RYBACH). Springer Verlag, Heidelberg-Berlin-New York, 191–196.

BRINK, H.-J., BURRI, P., LUNDE, A. & WINHARD, H. 1992: Hydrocarbon habitat and potential of Swiss and German Molasse Basin: A comparison. Ecologae geol. Helv. 85, 715–732.

BUNTEBARTH, G. 1979: Eine empirische Methode zur Berechnung von paläogeothermischen Gradienten aus dem Inkohlungsgrad organischer Einlagerungen in Sedimentgesteinen mit Anwendung auf den mittleren Oberrheingraben. Fortschr. Geol. Rheinld. u. Westf. 27, 97–108.

BUSTIN, R. M., BARNES, M. A. & BARNES, W. C. 1985: Diagenesis 10. Quantification and modelling of organic diagenesis. Geosci. Canada 12, 4–21.

CERMÁK, V. 1979: Heat Flow Map of Europe. In: Terrestrial heat flow in Europe (Ed. by V. CERMÁK & L. RYBACH). Springer Verlag, Heidelberg-Berlin-New York, 3–40.

CREANEY, S. 1980: The organic petrology of the Upper Cretaceous Boundary Creek formation, Beaufort-Mackenzie Basin. Bull. Canad. Petrol. Geol. 28, 112–119.

DEBEGLIA, N. & GABLE, R. 1984: Socle, écorché anté-triasique. In: Synthèse géologique du Sud-Est de la France (Ed. by J. DEBRAND-PASSARD & S. COURBOULEIX), carte G3, Mém. Bur. Rech. géol. min. 126.

DEICHMANN, N. 1990: Seismizität der Nordschweiz 1987–1989, und Auswertung der Erdbebenserien von Günsberg, Läufelfingen und Zeglingen. Nagra techn. Ber. 90-46, Baden.

DIEBOLD, P., NAEF, H. & AMMANN, M. 1991: Zur Tektonik der zentralen Nordschweiz: Interpretation aufgrund regionaler Seismik, Oberflächengeologie und Tiefbohrungen. Nagra techn. Ber. 90-04, Baden.

DOEBL, F., HELING, D., HOMANN, W., KARWEIL, J., TEICHMÜLLER, M. & WELTE D. 1974: Diagenesis of Tertiary clayey sediments and included dispersed organic matter in relationship to geothermics in the Upper Rhine Graben. In: Approaches to taphrogenesis (Ed. by J. H. ILLIES & K. FUCHS). Inter-Union Commission on Geodynamics, Scientific Report No. 8, E. Schweizerbart'sche Verlagsbuchhandlung, Stuttgart, 192–207.

DURAND, B., ALPERN, B., PITTION, J. L. & PRADIER, B. 1986: Reflectance of vitrinite as a control of thermal history of sediments. In: Thermal Modeling in Sedimentary Basins (Ed. by J. BURRUS). 1st IFP Exploration Research Conference, Carcans, France, June 3–7, 1985, Editions Technip, Paris 441–474.

ESPITALIÉ, J., DEROO, G. & MARQUIS, F. 1985a: La pyrolyse rock-eval et ses applications, première partie. Rev. Inst. Franc. Pétr. 40, 563–579.

– 1985b: La Pyrolyse rock-eval et ses applications, deuxième partie. Rev. Inst. Franç. Pétr. 40, 755–784.

– 1986: La pyrolyse rock-eval et ses applications, troisième partie. Rev. Inst. Franç. Pétr. 41, 73–89.

GORIN, G. E. & FEIST-BURKHARDT, S. 1990: Organic facies of Lower to Middle Jurassic sediments in the Jura Mountains, Switzerland. Rev. Paleobot. and Palynol. 65, 349–355.

GRIESSER, J.-C. & RYBACH, L. 1989: Numerical thermohydraulic modeling of deep groundwater circulation in crystalline basement: An example of calibration. In: Hydrogeological regimes and their subsurface thermal effects (Ed. by A. E. BECK, G. GARVEN & L.STEGENA). Geophysical Monograph 47, IUGG Vol. 2, Washington, 65–74.

HITCHON, B. 1984: Geothermal gradients, hydrodynamics, and hydrocarbon occurrences, Alberta, Canada. Bull. amer. Assoc. Petroleum Geol. 68, 713–743.

HOCHULI, P. A. 1978: Palynologische Untersuchungen im Oligozän und Untermiozän der Zentralen und Westlichen Paratethys. Beitr. Paläont. Oesterr. 4, 1–132.

HOOD, A. GUTJAHR, C. C. M. & HEACOCK, R. L. 1975: Organic metamorphism and the generation of petroleum. Bull. amer. Assoc. Petroleum Geol. 59, 986–996.

ILLIES, J. H. 1974: Intra-Plattentektonik in Mitteleuropa und der Rheintalgraben. Oberrh. geol. Abh. 23, 1–24.

– 1975: Intraplate tectonics in stable Europe as related to plate tectonics in the Alpine system. Geol. Rdsch. 64, 677–699.

– 1977: Ancient and recent rifting in the Rhinegraben. Geol. en Mijnb. 56, 329–350.

KÄLIN, B., RYBACH, L. & KEMPTER, E. H. K. 1992: Rates of deposition, uplift and erosion in the Swiss Molasse basin, estimated from sonic- and density-logs. Bull. Ver. schweiz. Petroleum-Geol. u. -Ing. 58/133, 9–22.

KARWEIL, J. 1956: Die Metamorphose vom Standpunkt der physikalischen Chemie. Z. dtsch. geol. Ges. 107, 132–138.

KELLER, B., BLÄSI, H.-R., PLATT, N. H., MOZLEY, P. S. & MATTER, A. 1990: Sedimentäre Architektur der distalen Unteren Süsswassermolasse und ihre Beziehung zur Diagenese und den petrophysikalischen Eigenschaften am Beispiel der Bohrung Langenthal. Nagra techn. Ber. 90-41, Baden.

KEMPTER, E. H. K. 1987: Fossile Maturität, Paläothermogradienten und Schichtlücken in der Bohrung Weiach im Lichte von Modellberechnungen der thermischen Maturität. Eclogae geol. Helv. 80, 543–552.

LACOMBE, O., ANGELIER, J., BERGERAT, F. & LAURANT, PH. 1990: Tectoniques superposées et perturbations de contrainte dans la zone transformante Rhin-Saône: apport de l'analyse des failes et des macles de la calcite. Bull. Soc. géol. France (8), 6/5, 853–863.

LAUBSCHER, H. P. 1974: Basement uplift and decollement in the Molasse Basin. Eclogae geol. Helv. 67, 531–537.

– 1982: Die Südostecke des Rheintalgrabens – ein kinematisches und dynamisches Problem. Eclogae geol. Helv. 75, 101–116.

– 1986: The eastern Jura: Relation between thin-skinned and basement tectonics, local and regional. Geol. Rdsch. 75, 535–553.

– 1987: Die tektonische Entwicklung der Nordschweiz. Eclogae geol. Helv. 80, 287–303.

– 1992: Jura kinematics and the Molasse Basin. Eclogae geol. Helv. 85, 653–675.

LEMCKE, K. 1974: Vertikalbewegungen des vormesozoischen Sockels im nördlichen Alpenvorland vom Perm bis zur Gegenwart. Eclogae geol. Helv. 67, 121–133.

– 1988: Geologie von Bayern: I. Das bayerische Alpenvorland vor der Eiszeit. Erdgeschichte – Bau – Bodenschätze. E. Schweizerbart'sche Verlagsbuchhandlung, Stuttgart.

LERCHE, I., YARZAB, R. F. & KENDALL, C. G. ST. C. 1984: Determination of paleoheat flux from vitrinite reflectance data. Bull. amer. Assoc. Petroleum Geol. 68, 1704–1717.

LINIGER, H. 1925: Geologie des Delsberger Beckens und der Umgebung von Movelier. Beitr. Geol. Karte Schweiz [N. F.] 55/4.

LO, H. B. 1992: Identification of indigenous vitrinites for improved thermal maturity evaluation. Org. Geochemistry 18, 359–364.

LOPATIN, N. V. 1971: Temperature and geologic time as factors in coalification. Akad. Nauk. SSSR, ser. geol. Izvestiya 3, 95–106.

LOUP, B. 1992a: Evolution de la partie septentrionale du domaine helvétique en Suisse occidentale au Trias et au Lias: contrôle par subsidence thermique et variations du niveau marin. Publ. Dépt. Géol. Paléont. 12, Université de Genève, Thèse N° 2508, Genève.

– 1992b: Mesozoic subsidence and stretching models of the lithosphere in Switzerland (Jura, Swiss Plateau and Helvetic realm). Eclogae geol. Helv. 85, 541–572.

MARCHIONI, D. L. 1983: The detection of weathering in coal by petrographic, rheologic and chemical methods. Int. J. Coal Geol. 2, 231–259.

MATTER, A., PETERS, T., ISENSCHMID, C., BLÄSI, H.-R. & ZIEGLER, H.-J. 1987: Sondierbohrung Riniken – Geologie, Textband. Nagra techn. Ber. 86-02, Baden.

MATTER, A., PETERS, T., BLÄSI, H.-R., MEYER, J., ISCHI, H. & MEYER, C. 1988a: Sondierbohrung Weiach – Geologie, Textband. Nagra techn. Ber. 86-01, Baden.

MATTER, A., PETERS, T., BLÄSI, H.-R., SCHENKER, F. & WEISS, H.-P. 1988b: Sondierbohrung Schafisheim – Geologie, Textband. Nagra techn. Ber. 86-03, Baden.

MEIER, R., HURTIG, E. & LUDWIG, A. 1979: Fault tectonics and heat flow in Europe. In: Terrestrial heat flow in Europe (Ed. by V. CERMÁK & L. RYBACH). Springer Verlag, Heidelberg-Berlin-New York, 112–118.

MONNIER, F. 1982: Thermal diagenesis in the Swiss Molasse basin: implications for oil generation. Canad. J. Earth Sci. 19, 328–342.

MORGAN, P. 1982: Heat flow in rift zones. In: Continental and oceanic rifts (Ed. by G. PALMASON). Amer. Geoph. Union, Geodyn. Ser. 8, 107–122.

MÜLLER, W. H., HUBER, M., ISLER, A. & KLEBOTH, P. 1984: Erläuterungen zur geologischen Karte der zentralen Nordostschweiz 1:100000. Nagra techn. Ber. 84-25, Baden.

MULLIS, J. 1987: Fluideinschluss-Untersuchung in den Nagra-Bohrungen der Nordschweiz. Eclogae geol. Helv. 80, 553–568.

NAEF, H., DIEBOLD, P. & SCHLANKE, S. 1985: Sedimentation und Tektonik im Tertiär der Nordschweiz. Nagra techn. Ber. 85-14, Baden.

NAGRA 1988: Sedimentstudie – Zwischenbericht 1988: Möglichkeiten zur Endlagerung langlebiger radioaktiver Abfälle in den Sedimenten der Schweiz. Nagra techn. Ber. 88-25, Baden.

NESBITT, B. E. 1990: Short course on fluids in tectonically active regimes of the continental crust. Min. Ass. of Canada, Short Course Handbook 18, Vancouver.

OLIVER, J. 1986: Fluids expelled tectonically from orogenic belts: Their role in hydrocarbon migration and other geologic phenomena. Geology 14, 99–102.

PERSON, M. & GARVEN, G. 1992: Hydrologic constraints on petroleum generation within continental rift basins: Theory and application to the Rhine Graben. Bull. amer. Assoc. Petroleum Geol. 76, 468–488.

PRICE, L. C. 1983: Geologic time as a parameter in organic metamorphism and vitrinite reflectance as an absolute paleogeothermometer. J. Petroleum. Geol. 6, 5–38.

RAMSEYER, K. 1987: Diagenese des Buntsandsteins und ihre Beziehung zur tektonischen Entwicklung der Nordschweiz. Eclogae geol. Helv. 80, 383–395.

ROBERT, P. 1985: Histoire géothermique et diagenèse organique. Bull. Cent. Rech. Explor.-Prod. Elf-Aquitaine, Mém. 8, Pau.

RYBACH, L. 1984: The paleogeothermal conditions of the Swiss molasse basin: implication for hydrocarbon potential. Rev. Inst. Franç. Pétr. 39, 143–146.

RYBACH, L., EUGSTER, W. & GRIESSER, J.-C. 1987: Die geothermischen Verhältnisse in der Nordschweiz. Eclogae geol. Helv. 80, 521–534.

SCHAER, J.-P. 1992: Tectonic evolution and vertical movement in Western Switzerland. Eclogae geol. Helv. 85, 695–699.

SCHEGG, R. 1992a: Coalification, shale diagenesis and thermal modelling in the Alpine Foreland Basin: The Western Molasse Basin (Switzerland, France). Org. Geochemistry 18, 289–300.

– 1992b: Thermal maturity of the Swiss Molasse Basin: Indications for paleogeothermal anomalies? Eclogae geol. Helv. 85, 745–764.

– 1993: Thermal maturity and modelling of sediments in the North Alpine Foreland Basin (Switzerland, France). Publ. Dépt. Géol. Paléont. 15, Université de Genève, Thèse N° 2612, Genève.

SINCLAIR, H. D., COAKLEY, B. J., ALLEN, P. A. & WATTS, A. B. 1991: Simulation of foreland basin stratigraphy using a diffusion model of mountain belt uplift and erosion: an example from the Central Alps, Switzerland. Tectonics 10, 599–620.

STACH, E., MACKOWSKY, M.-TH., TEICHMÜLLER, M. R., TAYLOR, G. H. & CHANDRA, D. 1982: Stach's textbook of coal petrology. 3. ed., Gebrüder Bornträger, Berlin-Stuttgart.

SUGGATE, R. P. 1982: Low-rank seuqences and scales of organic metamorphism. J. Petroleum Geol. 4, 377–392.

SUTER, M. 1978: Geologische Interpretation eines reflexionsseismischen W-E-Profils durch das Delsberger Becken (Faltenjura). Eclogae geol. Helv. 71, 267–275.

SWEENEY, J. J. & BURNHAM, A. K. 1990: Evaluation of a simple model of vitrinite reflectance based on chemical kinetics. Bull. amer. Assoc. Petroleum Geol. 74, 1559–1570.

TEICHMÜLLER, M. 1979: Die Diagenese der kohligen Substanzen in den Gesteinen des Tertiärs und Mesozoikums des mittleren Oberrhein-Grabens. Fortschr. Geol. Rheinld. u. Westf. 27, 19–49.

TEICHMÜLLER, M. & OTTENJANN, K. 1977: Art und Diagenese von Liptiniten und lipoiden Stoffen in einem Erdölmuttergestein auf Grund fluoreszenzmikroskopischer Untersuchungen. Erdöl und Kohle 30, 387–398.

TEICHMÜLLER, M. & TEICHMÜLLER, R. 1979: Zur geothermischen Geschichte des Oberrheingrabens. Zusammenfassung und Auswertung eines Symposiums. Fortschr. Geol. Rheinld. u. Westf. 27, 109–120.

TEICHMÜLLER, R. & TEICHMÜLLER, M. 1986: Relations between coalification and paleogeothermics in Variscan and Alpidic foredeeps of western Europe. In: Lecture Notes in Earth Sciences, Vol. 5, Paleogeothermics (Ed. by G. BUNTEBARTH & L. STEGENA). Springer-Verlag, Berlin-Heidelberg, 53–78.

TISSOT, B. P., PELET, R. & UNGERER, PH. 1987: Thermal history of sedimentary basins, maturation indices and kinetics of oil and gas generation. Bull. amer. Assoc. Petroleum Geol. 71, 1445–1466.

TISSOT, B. P. & WELTE, D. H. 1984: Petroleum formation and occurrence. Springer-Verlag, Berlin, Heidelberg, New York, Tokyo.

TODOROV, I., SCHEGG, R. & CHOCHOV, S. 1992: Maturity studies in the Carboniferous Dobroudja coal basin (Northeastern Bulgaria)—coalification, clay diagenesis and thermal modelling. Int. J. Coal Geol. 21, 161–185.

TRÜMPY, R. 1980: Geology of Switzerland, part A. Wepf & Co. Publ., Basel, New York.

WAPLES, D. W. 1980: Time and temperature in petroleum formation: application of Lopatin's method to petroleum exploration. Bull. amer. Assoc. Petroleum Geol. 64, 916–926.

WELTE, D. H. & YALÇIN, M. N. 1988: Basin modelling—A new comprehensive method in petroleum geology. Org. Geochemistry 13, 141–151.

WERNER, D. & KAHLE, H.-G. 1980: A geophysical study of the Rhinegraben – I. Kinematics and geothermics. Geophys. J. R. Astr. Soc. 62, 617–629.

WILDI, W., FUNK, H., LOUP, B., AMATO, E. & HUGGENBERGER, P. 1989: Mesozoic subsidence history of the European marginal shelves of the alpine Tethys (Helvetic realm, Swiss Plateau and Jura). Eclogae geol. Helv. 82, 817–840.

WOLF, M. & HAGEMANN, H. W. 1987: Inkohlung und Geothermik in meso- und paläozoischen Sedimenten der Nordschweiz und Vergleich zu Inkohlungsdaten aus Süddeutschland. Eclogae geol. Helv. 80, 535–542.

ZIEGLER, P. A. 1987: Late Cretaceous and Cenozoic intra-plate compressional deformations in the Alpine foreland—a geodynamic model. Tectonophysics 137, 389–420.

– 1988: Evolution of the Arctic-North Atlantic and the Western Tethys. Mem. amer. Assoc. Petroleum Geol. 43.

– 1992: European Cenozoic rift system. Tectonophysics 208, 91–111.

CITED GEOLOGICAL MAPS

Geological map of Switzerland 1:25000, with explanation notes:
- Arlesheim (Blatt 1067)
- Mühlberg/Aarau, Geologische Spezialkarte 45
- Mühlberg/Hauensteingebiet, Geologische Spezialkarte 73

Comm. géol. Suisse, Basel

Manuscript received 5 November 1992
Revision accepted 1 June 1993